INTERNATIONAL JOURNAL OF CLIMATOLOGY
Int. J. Climatol. **31**: 1573–1583 (2011)
Published online 15 June 2010 in Wiley Online Library
(wileyonlinelibrary.com) DOI: 10.1002/joc.2184

RMetS
Royal Meteorological Society

Interannual to decadal changes in extreme fire weather event frequencies across the southwestern United States

Michael A. Crimmins*
Department of Soil, Water, & Environmental Science, The University of Arizona, Tucson, AZ 85721-0038, USA

ABSTRACT: Low-frequency changes (decades to years) in precipitation related to the El Niño-Southern Oscillation (ENSO) and the Pacific Decadal Oscillation (PDO) are known to influence wildfire variability across the southwest United States. Little work has been done to identify whether daily fire weather variability, also important to wildfire activity, is influenced by these same climatic phenomena. This study identifies the synoptic climatological conditions associated with extreme fire weather events in the Southwest and constructs an extreme fire weather frequency data set for the period of 1958–2003 using a logistic regression technique. Interannual changes in extreme fire weather day frequencies are not linearly correlated with either ENSO or PDO, but do show significant deviations from expected values when grouped by PDO phase (positive or negative) and further subgrouped by ENSO state (La Niña, El Niño or neutral). A higher number of extreme fire weather days occur during the negative phase of the PDO, especially when accompanied by a La Niña event. Copyright © 2010 Royal Meteorological Society

KEY WORDS wildfire; extreme events; decadal variability; Pacific Decadal Oscillation; El Niño-Southern Oscillation; fire weather

Received 20 January 2010; Revised 4 May 2010; Accepted 6 May 2010

1. Introduction

Climatological connections to wildfire variability exist through a variety of mechanisms operating on different temporal scales. Low-frequency (years to decades) changes in precipitation regimes that modulate fuel production and fuel conditioning have been linked to wildfire variability in several studies (Simard *et al*., 1985; Swetnam and Betancourt, 1990, 1998; Westerling and Swetnam, 2003; Crimmins and Comrie, 2004; Littell *et al*., 2009). Shorter term (days to weeks) changes in synoptic circulation regimes have also been identified as important climatological influences on wildfire activity (Brotak and Reifsnyder, 1977; Johnson and Wowchuk, 1993; Nash and Johnson, 1996; Flannigan *et al*., 2003; Westerling *et al*., 2004). Changes in daily fire weather conditions (wind speed, temperature and relative humidity) that occur through low-frequency teleconnection patterns all are climatic components related to wildfire variability. Little work has been done to examine how these components are connected and how they may co-vary through time.

The relationship between wildfire and climate across the southwest United States involves an interesting interaction between wet and dry cycles that evolves over many seasons and years. Identified fire–climate relationships in areas of Arizona and New Mexico dominated by xerophytic forests show that antecedent climate conditions months to years prior to fire seasons can be as important as the actual fire season conditions (Swetnam and Betancourt, 1998; Crimmins and Comrie, 2004). Peak fire season (April, May and June) conditions are climatologically hot and dry across Arizona and New Mexico. Above normal temperatures and below normal precipitation would do little to change already harsh conditions during the spring. Precipitation anomalies in seasons to years prior appear to promote the growth and accumulation of fine fuels that exacerbate wildfire activity during the fire season. Several studies have shown that the sequencing of El Niño events (wet) and La Niña events (dry) can promote the growth of fuels and then subsequently dry them out over a period of years (Swetnam and Betancourt, 1990, 1998; Crimmins and Comrie, 2004).

Short-term transitions to synoptic patterns that promote extreme fire weather conditions are also important in controlling seasonal wildfire variability across the southwest United States. A discrete synoptic pattern characterized by a strong geopotential height gradient and broad southwest flow across the Southwest can elevate fire danger by bringing extremely windy conditions and low-relative humidity values to the region (Schroeder, 1969; Crimmins, 2006). Wind events that occur during the spring fire season are particularly dangerous due to the background hot and dry conditions. Wildfires can quickly grow to large sizes when coincident with these wind events (e.g. Cerro Grande Wildfire; Crimmins, 2006).

* Correspondence to: Michael A. Crimmins, Department of Soil, Water, & Environmental Science, The University of Arizona, Room 429, Shantz Building #38, P.O. Box 210038, Tucson, AZ 85721-0038, USA. E-mail: crimmins@email.arizona.edu

This study examines the interannual changes in extreme fire weather event frequencies with respect to known teleconnective phenomena already identified as important to southwestern United States climatic variability [e.g. El Niño-Southern Oscillation (ENSO); Redmond and Koch, 1991 and PDO; McCabe and Dettinger, 1999]. An extension of the record of extreme fire weather frequencies is constructed using synoptic circulation indices and logistic regression modelling. Increasing the period of record strengthens the analysis of interannual variability in extreme fire weather frequencies. Identification of interannual trends in extreme fire weather frequencies will help improve our understanding of the connections between climatic and wildfire variabilities across the southwest United States.

2. Data and methods

2.1. Extreme fire weather days

The daily fire danger ratings used as predictands in the logistic regression model were calculated from daily weather observations at 15 Remote Automated Weather Stations (RAWS; Figure 1). Initially, 33 stations from across Arizona and New Mexico were considered for inclusion in this study. Short periods of record and missing data forced the exclusion of 18 stations. The final 15 stations included in this study represent the best spatial coverage of stations for the period of 1988–2003.

Daily fire danger levels were determined by calculating the daily Fosberg Fire Weather Index (FFWI) values for each of the 15 stations. Maximum daily temperature, minimum daily relative humidity and daily average wind speed were used from daily RAWS weather summaries to create daily FFWI values at each station. This index is essentially a nonlinear filter that is extremely sensitive to changes in wind speed and relative humidity levels (Fosberg, 1978; Goodrick, 2002; Crimmins, 2006). High winds and low-relative humidity values result in high-FFWI values (Fosberg, 1978). A statistical study by Haines *et al*. (1983) found the FFWI to be a strong and significant predictor of wildfire activity when compared with historical records in the northeastern United States. The daily FFWI values from the 15 RAWS sites were combined into one regional time series by first converting the individual station time series into z-scores and then averaging them. It is understood that averaging the individual time series created a loss of information, but the regional signal was the desired component of the variability in daily fire danger. Sub-regional variability in daily fire danger does exist, but it is not addressed in this study.

The single, regional time series of FFWI z-scores was converted to rank-percentiles with the highest values being the highest percentiles. The 90th percentile was chosen as the break point to determine extreme fire weather conditions. This is a common threshold used by the fire management community to identify extreme fire weather conditions (Fosberg *et al*., 1993; Schlobohm and Brain, 2002). The final time series used as the predictand in the logistic regression model consisted of a binary variable indicating occurrence (1) or non-occurrence (0) of an exceedance of the 90th percentile threshold.

2.2. Reanalysis data

Time series of daily ($18z$) reanalysis data were extracted and used as predictors in the logistic regression model. The $18z$ time step was used from the four-time daily data

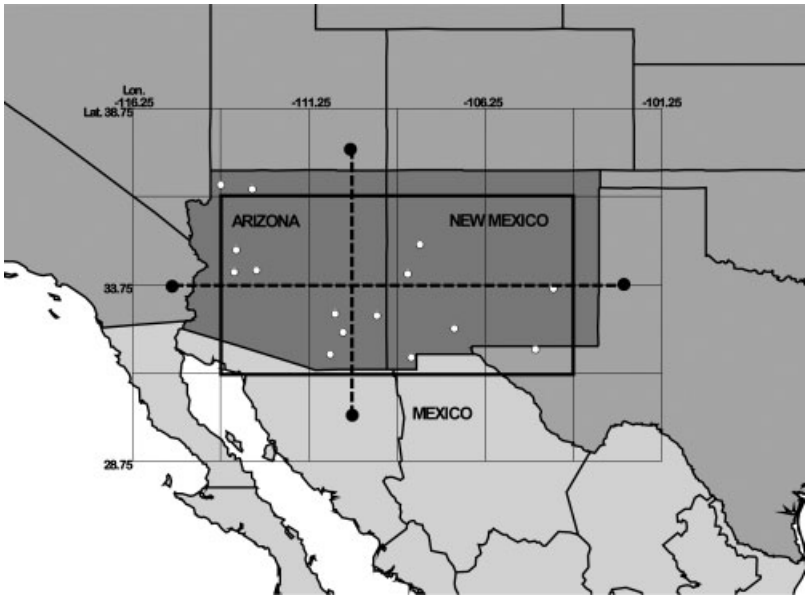

Figure 1. Study area with RAWS sites in Arizona and New Mexico shown (white circles). Grid (thin lines) represents the location of reanalysis data points (centre of grid cells). Dashed lines divide where North–South and East–West gradient time series were developed (black circles). Dark outline of grid cells over Arizona and New Mexico highlights reanalysis data points used in calculation of average regional relative humidity time series.

set to coincide with maximum temperatures and minimum relative humidity values occurring in the afternoon across the southwest United States. Monthly average grids were used to develop geopotential height anomaly composites. Reanalysis data are produced by the National Center for Environmental Prediction and National Center for Atmospheric Research (Kalnay *et al*., 1996). These data represent model reconstructions of various atmospheric fields from daily observations at a grid resolution of 2.5°. They provide a spatially and temporally consistent global data set and are widely used in all types of climatological studies. The time series use 700 mb level variables because of their proximity to the higher elevation areas of the Southwest. The study period was confined to the period of 1958–2003, when confidence in reanalysis variable fields is highest (Kalnay *et al*., 1996).

2.3. Logistic regression modelling

A logistic regression model was used to construct an extended record of daily extreme fire weather frequencies back to 1958. The observational record of the current fire weather-monitoring network only extends back to the late 1980s and is not sufficient for long-term climatological analyses. Model specification was done with reanalysis grid time series to capture upper level (700 mb) circulation characteristics important to driving to surface fire weather conditions. Several studies have identified synoptic circulation patterns that are associated with extreme, surface fire weather conditions (Schroeder, 1969; Brotak and Reifsnyder, 1977; Johnson and Wowchuk, 1993; Takle *et al*., 1994; Crimmins, 2006). Figure 2 shows a 700-mb geopotential height anomaly composite of 141 extreme fire weather days occurring in April, May and June for the period of 1988–2003. A steep geopotential height gradient and anomalously low-relative humidity characterize the synoptic environment over the study area during these extreme fire weather days. Three components were used to capture this synoptic signature in the regression model. A North–South geopotential height gradient, East–West height gradient and regional average relative humidity (Figure 1) were used as predictors to predict the occurrence or non-occurrence of a 90th-percentile exceedance day. Daily odds-ratio values produced by the logistic regression model were examined to determine exceedance days. Days with odds-ratio values greater than 0.5 were counted as exceedance days. Final output consists of monthly (April, May and June) totals of predicted exceedance days for the period of 1958–2003.

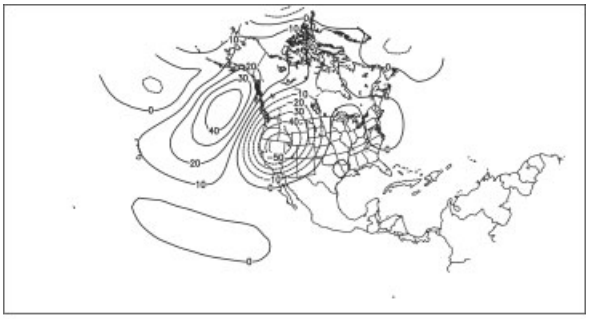

700mb geopotential height anomaly (contour interval: 10m)

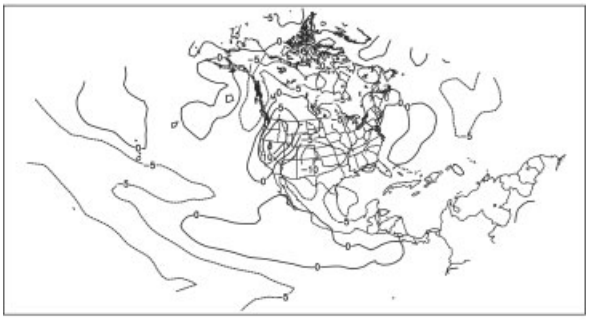

700mb relative humidity anomaly (contour interval: 5%)

Figure 2. Anomaly composites of all FFWI 90th percentile exceedance days in AMJ from 1988 to 2003 ($n = 141$ days).

2.4. Pacific sea surface temperature indices

Relationships between extreme fire weather event frequencies and ENSO and PDO variability were examined through the use of sea surface temperature (SST) indices. The PDO index developed by Mantua *et al*. (1997) was used to characterize the state of the North Pacific region. Index values represent the leading principal component of monthly North Pacific SST variability (Mantua *et al*., 1997). The Oceanic Niño Index (ONI) was used to capture the state of the equatorial region of the Pacific Ocean. The ONI is a 3-month running mean of the extended reconstructed SST (ERSST.v2) anomalies from the Niño3.4 region (5°N–5°S, 120–170°W) based on the 1971–2000 base period Climate Prediction Center (CPC), 2010. Trenberth (1997) proposed the use of Niño3.4 SSTs as a standard measure of ENSO variability because it most effectively captures the Pacific warm pool during El Niño events.

Both the ONI and the PDO are SST-based indices ensuring commensurate persistence and atmospheric response time lags. The assumption is that these SST-based indices will reflect changes in forcing mechanisms that will eventually affect atmospheric circulation and afford forecasting lead times. This is done as an alternative to using the traditional atmospheric circulation indices associated with ENSO and PDO [Southern Oscillation Index (SOI) and North Pacific Index (NP)]. The atmospheric circulation index values are highly correlated with the SST-based index values when lagged by one season. December–January–February (DJF) ONI values were correlated with March–April–May (MAM) SOI values at $r = -0.897$, whereas DJF PDO and MAM NP values were correlated at -0.687.

Spearman rank (ρ) correlations, χ^2 tests and anomaly composites were all used to assess relationships between the SST indices and the frequency of extreme fire weather events. The local statistical significance of composite anomaly patterns was determined using the bootstrapping percentile method (Efron and Tibshirani, 1993). Each composite grid cell was resampled with replacement 400 times to develop an artificial distribution. Significant

differences of the anomaly from 0 (no anomaly) were then determined at the 0.1 and 0.05 levels.

3. Results and discussion

3.1. Extreme fire weather frequency modelling

Three time series derived from reanalysis data points were used to specify the logistic regression model. A composite of 700 mb geopotential height anomalies and relative humidity anomalies for 141 April–May–June (AMJ) FFWI 90th percentile exceedance days was developed to determine the circulation anomaly associated with critical fire weather days (Figure 2). This pattern is consistent with other studies of critical fire weather patterns across the southwest United States (Schroeder, 1969; Crimmins, 2006). Examination of the geopotential and relative humidity anomalies in Figure 2 shows a steep geopotential height gradient and negative relative humidity anomaly across Arizona and New Mexico. North–South and East–West gradient values were entered into the logistic regression model to capture variations in this geopotential height gradient pattern and a regional average relative humidity was used to discriminate variations in daily humidity anomalies (Figure 1). The parameter estimates of these three variables were all highly significant ($p < 0.001$) and the overall model was highly significant ($p < 0.001$) indicating that the model was well specified. The receiver operating characteristic (ROC) curve produced an 'Area Under Curve' value of 0.93281 indicating that the model is well balanced between producing a low number of false positive values relative to false negative values at a range of probability thresholds (Swets, 1988).

The model is well specified, but does not perfectly fit the input data. A pseudo-R^2 value can be calculated relative to an idealized, saturated model but does not represent percent variance explained like a traditional R^2 value. This model has an R^2 value of 0.45, which represents a reasonable fit. A threshold probability of 0.50 was used to determine the occurrence of an exceedance day. This appears to be a reasonable threshold upon the examination of the predicted *versus* observed frequencies (Figure 3). Even with a relatively low threshold probability, the model tends to underpredict yearly exceedance frequencies when AMJ are considered together (Figure 3). Closer examination of the individual months shows that the model performs the best for the month of May. The correlations (r) between observed and predicted exceedance day frequencies for April, May and June were 0.35, 0.91 and 0.45, respectively. Only the May correlation ($r = 0.91$) was significant ($p < 0.001$). The fact that the May exceedance day prediction model performs best could be due to the regional-scale nature of the analysis. Complex patterns in moisture and storm tracks from late winter storms in April and early season monsoon moisture incursions in

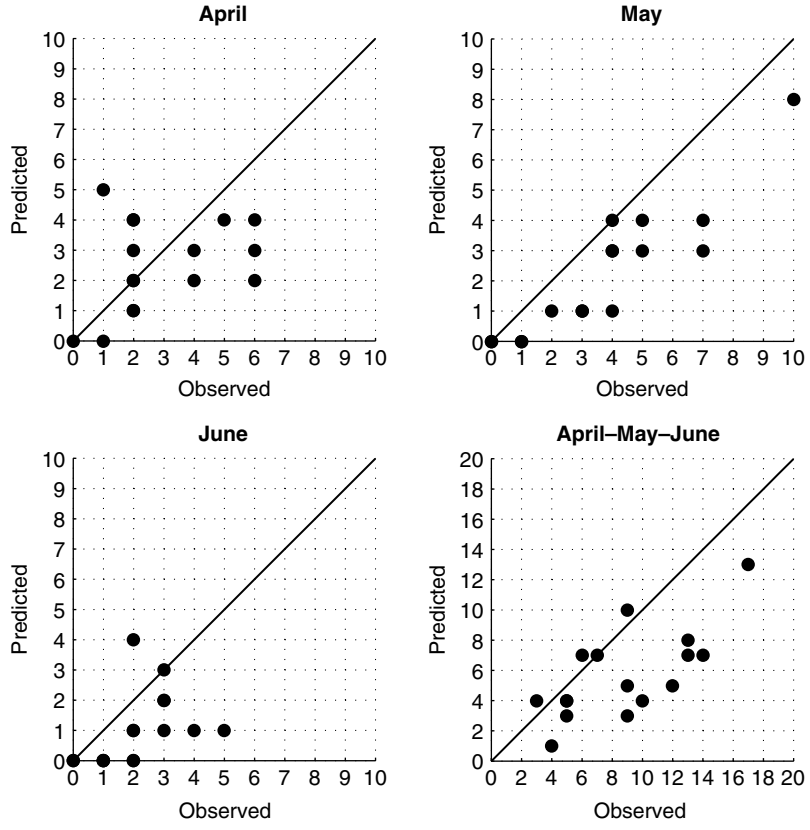

Figure 3. Observed *versus* predicted exceedance day frequencies between 1988 and 2001 ($n = 14$, identical values in some years are plotted as one point).

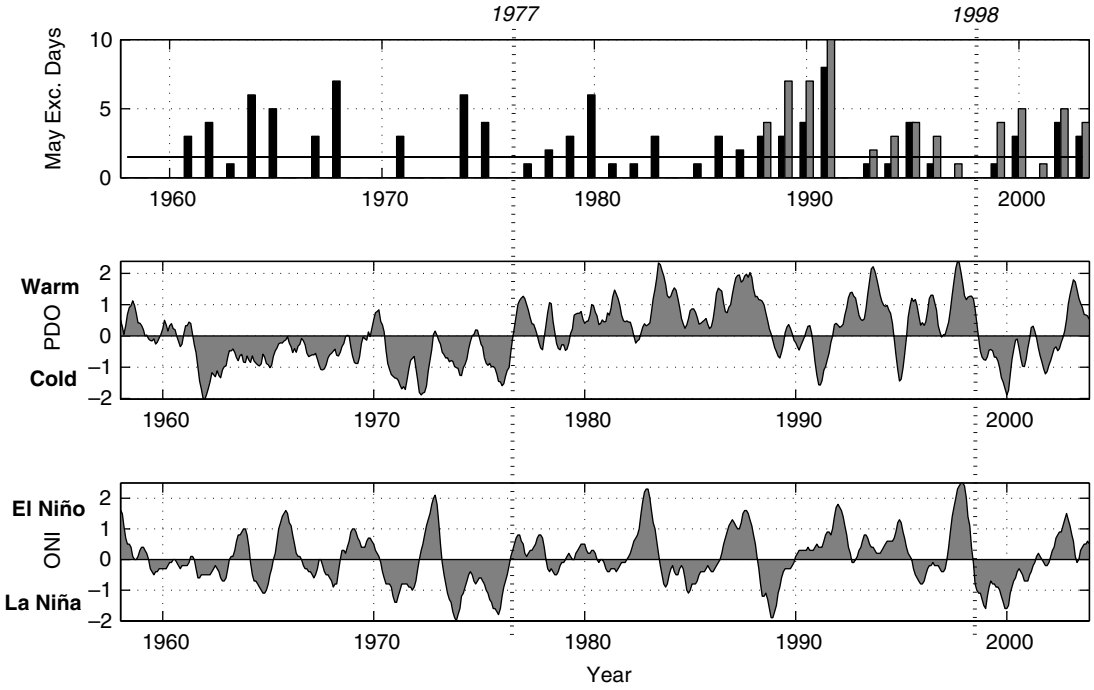

Figure 4. Actual (grey bars) and reconstructed (black bars) May exceedance day frequencies (top), monthly ONI (middle) and PDO (5-month running average, bottom) values. Dashed vertical lines represent major shifts in North Pacific sea surface temperature patterns.

June can impact different parts of the region, weakening the coherence of the regional, surface-based exceedance day signal and connection to synoptic scale circulation features. Surface conditions are most likely to be similar across all stations during the month of May (all climatologically dry and warm) and would most likely be connected to synoptic conditions in a coherent manner. Model confidence is highest for May days and most exceedance days occur during May (43% of total AMJ exceedance days), so subsequent analyses will be confined to the month of May.

Modelled May exceedance day frequencies for 1958–2003 are shown in Figure 4, along with monthly Pacific Decadal Oscillation (PDO) index and ONI values. Frequencies are highly variable with values ranging from 0 to 8 exceedance days over the 46-year study period. The median value is 1.5 and the range is 8, indicating substantial positive skew.

Subtle patterns are evident when comparing the May exceedance day frequencies with the PDO time series (Figure 4). PDO values were generally negative for the early part of the record with a shift towards positive values occurring around 1976–1977. Two substantial but short-lived shifts to negative PDO values occurred in 1989 and 1999 during the latter part of the record from 1977 to 2003. May exceedance day values were highly variable during the negative PDO phase from 1962 to 1976. This period had some of the highest predicted exceedance day frequencies for the entire study period but also had 6 years with zero predicted exceedance days. The shift to positive PDO values in 1976 marked a period of lower variability and also lower exceedance day values. May exceedance day frequencies never increase higher than 3 days from 1981 to 1989. The shift to negative PDO values from 1989 to 1991 was accompanied by dramatic increases in predicted exceedance day frequencies.

The above discussion relates interannual variability in North Pacific SSTs with changing frequencies of May extreme fire weather days. Well-known teleconnection patterns originating from equatorial SST anomalies impact winter temperature and precipitation across the southwest United States (Redmond and Koch, 1991; Gershunov, 1998; Cayan *et al*., 1999; Sheppard *et al*., 2002). These teleconnections appear to be limited to the winter season for temperature and precipitation, but may extend into the spring and modulate the occurrence of critical fire weather circulation patterns. Transitions between El Niño (positive ONI) and La Niña (negative ONI) conditions occur about every 4 years during the early period from 1961 to 1976 (Figure 4). These transitions may help explain the high variability in exceedance day frequencies from year to year during the same period. The pattern of high- and low-exceedance day counts during the early part of the record may be related to ENSO-induced atmospheric teleconnections.

3.2. χ^2 testing of group frequencies

No significant correlations were found when Spearman rank correlations were calculated between May exceedance day frequencies and seasonally averaged ONI and PDO indices (prior winter and spring season including May). The patterns in Figure 4 however still suggest a relationship between the data sets. There may be nonlinear interactions that will not be resolved by a linear

Table I. Composite group memberships by PDO phase and ENSO state (1958–2003).

	PDO positive	PDO negative
El Niño	1958, 1992, 1978, 1983, 1970, 1977, 1998, 1988, 2003, 1987	1969, 1964, 1995, 1966, 1973
La Niña	2001, 1996, 1985, 1984	1972, 1962, 1976, 1971, 1974, 2000, 1965, 1989, 1999, 1968, 1975
Neutral	1997, 1961, 1960, 1982, 1980, 1993, 1981, 1986, 1994	1991, 1967, 2002, 1963, 1990, 1979, 1959

correlation analysis. An alternative analysis is to evaluate the general state that each index is portraying (e.g. El Niño, neutral or La Niña) and form categories. This method was used by Gershunov and Barnett (1998) to develop sea level pressure composites of general PDO and ENSO states. A similar approach was used in this study to evaluate the frequency of May exceedance days by PDO phase, ENSO state and subgroups representing the combination of both (e.g. PDO+ and El Niño). The groupings are shown in Table I. ENSO and PDO states from the winter months preceding the May in the question are used. This was done with the expectation that changes in SST reflected by the indices would take time to manifest atmospheric circulation anomalies into the spring and that the SST anomalies would persist into spring. Evaluating the lagged relationship between the SST states and the May exceedance frequencies also affords a potential forecasting tool. If relationships exist, the winter SST state could be used to project the potential extreme fire weather activity for the upcoming spring. El Niño and La Niña events are based on the CPC method of a 0.5-°C threshold in the ONI during the winter months of DJF, where La Niña events are $>-0.5\,^{\circ}$C and El Niño events are $>0.5\,^{\circ}$C (CPC, 2004). PDO state is based on average values during a longer 5-month season [November-December-January-February-March (NDJFM)] centred on the winter months to represent the persistent, lower variability component of the monthly index values consistent with the approach taken by Mantua *et al*. (1997) and Hidalgo and Dracup (2003).

χ^2 tests were performed between the expected and observed proportions of exceedance to non-exceedance days for several different groupings based on ENSO and PDO states (Table II). The total number of observed May exceedance days for both PDO states was significantly ($p < 0.01$) different from the expected number. Fewer than expected occurred during Mays where the winter PDO was positive and more than expected occurred during the negative PDO state. None of the ENSO-based groupings had significant deviations of the observed *versus* expected frequencies. The observed frequencies were higher than expected during La Niña events and were lower during El Niño events, but not significantly different. Grouping on ENSO and PDO states together helped to further discriminate the relationship between May exceedance days and Pacific Ocean states. Two subgroups had differences in observed and expected frequencies that were highly significant ($p < 0.05$). Interestingly, they were both La Niña events but associated with different PDO states. Mays associated with La Niña events during PDO+ had a less than expected number of days, whereas La Niña-PDO− had more. Neutral-PDO− also had more days than expected contributing to the overall relationship between PDO− and higher exceedance day frequencies. El Niño-PDO+ had fewer than the expected days helping to explain the PDO+/fewer exceedance day relationship.

These results suggest that Mays that follow PDO− winters had a higher frequency of extreme fire weather days, especially if a La Niña event was underway. The opposite was true for Mays that were preceded by PDO+ winters and both El Niño and La Niña events. ENSO and PDO states have rarely been implicated in explaining springtime climatic variability across the southwestern United States. The strongest teleconnection patterns in the southwest United States associated with ENSO and PDO are found during the winter with precipitation and temperature (Gershunov and Barnett, 1998; Gutzler *et al*., 2002; Brown and Comrie, 2004). This study deals with very subtle changes in extreme fire weather events that most likely would have very little influence on mean monthly climate values. The relationships identified in above the χ^2 analyses are not evident when examined with linear methods like correlation analysis.

3.3. Composite analysis

A composite analysis was performed to examine circulation anomalies that may help explain the shifts in May

Table II. χ^2 tests of the observed *versus* the expected number of May exceedance days based on the composite group.

	Observed	Expected	χ^2 value (p)
PDO+	32	50.5	6.91 (0.009)
PDO−	69	50.5	6.91 (0.009)
EN	24	32.9	2.36 (0.124)
LN	38	32.9	0.66 (0.417)
NE	39	35.1	0.38 (0.538)
PDO+/EN	14	22	2.76 (0.096)
PDO+/LN	2	8.8	4.83 (0.028)
PDO+/NE	16	19.8	0.59 (0.442)
PDO−/EN	10	11	0.02 (0.888)
PDO−/LN	36	24.2	5.68 (0.017)
PDO−/NE	23	15.4	3.52 (0.06)

PDO, Pacific Decadal Oscillation; EN, El Niño; LN, La Niña; NE, neutral.

exceedance day frequencies associated with the different composite groups. Composites of monthly May 700 mb geopotential height anomalies for PDO+ and PDO− years are presented in Figure 5. The patterns are consistent with the results of the χ^2 test between the PDO+ and PDO− groups (Table II). A positive–negative–positive anomaly pattern is present on the PDO− composite, which is similar to the exceedance day composite presented in Figure 2. Crimmins (2006) found that a strong geopotential height gradient produced by deep troughs moving through the southwest United States produced the majority of dry, high wind events and extreme fire weather days during the springtime. A negative geopotential height anomaly across the western United States as presented in the exceedance day composite (Figure 2) and PDO− composite (Figure 5) would suggest an unusually strong trough pattern and height gradient across Arizona and New Mexico. The opposite pattern (negative–positive–negative anomaly) is present on the PDO+ composite. Patterns on both composites have significant anomaly areas, with the north-central United States having the most consistent anomaly area that is highly significant. The anomalies are weak, but do indicate a more favourable monthly pattern that would relate to discrete exceedance day events during PDO− than PDO+.

Subcomposites grouped by PDO and ENSO state are presented in Figure 6. The highly significant χ^2 value La Niña groups have highly significant geopotential height anomalies across the southwest United States. The La Niña-PDO− composite shows a pattern with anomalous positive geopotential height anomalies over the Pacific and negative anomalies over the western United States.

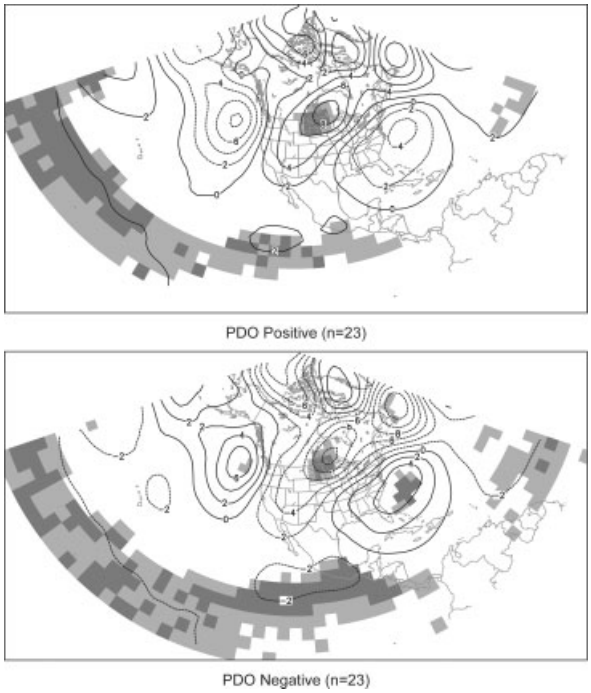

Figure 5. May 700 mb geopotential height anomalies based on the PDO phase grouping (solid lines, positive anomaly; dashed lines, negative anomalies; contour interval, 2 m). Dark shading indicates significance at 0.05 level and light shading indicates significance at 0.10 level.

This is consistent with the composite exceedance day geopotential height anomaly pattern depicted in Figure 2. The La Niña-PDO+ composite shows a very different pattern with significant positive geopotential height anomalies extending from the mid-Pacific into the southwest United States. This subgroup has a very small sample size of 4, but reflects a consistent pattern of anomalous positive geopotential heights across the southwest United States counter to the exceedance day pattern in Figure 2. The positive geopotential height anomaly La Niña-PDO+ subgroup is most likely indicative of years where a strong subtropical high dominated May weather across the western United States, blocking the troughing events necessary for extreme fire weather conditions across the Southwest (Crimmins, 2006).

The El Niño-PDO+ and Neutral-PDO− groups had weaker ($0.05 < p < 0.1$), but still notable χ^2 values. The El Niño-PDO+ composite shows a weak and generally insignificant anomaly pattern across the United States. A weak negative–positive geopotential height anomaly pattern can be made out, but only the upper mid-west has significantly positive geopotential height anomalies. The weak negative geopotential height anomaly off the California coast and positive anomalies over the north-central United States suggest a pattern that is counter to the western United States negative height anomaly associated with exceedance days. This group has a lower than the expected number of exceedance days, but the anomaly pattern is weak and does not indicate any very persistent features that would definitively explain the reduction in the observed exceedance days.

An opposite positive–negative–positive geopotential height anomaly pattern is present on the neutral-PDO− composite. Significant positive geopotential height anomalies are found over Alaska and the southeast United States with a very weak and insignificant negative height anomaly between these areas over the western United States. This group had 23 exceedance days relative to the 15.4 expected (χ^2; $p = 0.06$) and has a synoptic pattern similar to the exceedance day composite in Figure 2. The weak negative anomaly over the western United States suggests that deeper negative geopotential height anomalies and extreme fire weather days are associated with passing troughs rather than a persistent pattern over the entire month.

Both neutral-PDO+ and El Niño-PDO− had insignificant χ^2 values and anomaly patterns that are neither favourable nor unfavourable for producing exceedance days across the southwest United States. The neutral-PDO+ composite has a negative–positive–negative geopotential height anomaly pattern with significant negative geopotential height anomalies south of the Aleutian Islands off the Alaskan mainland and over the eastern United States. Weak, but significant, positive anomalies occur only in central Canada. No geopotential height anomalies exist over the southwest United States indicating a lack of persistent circulation features for this area.

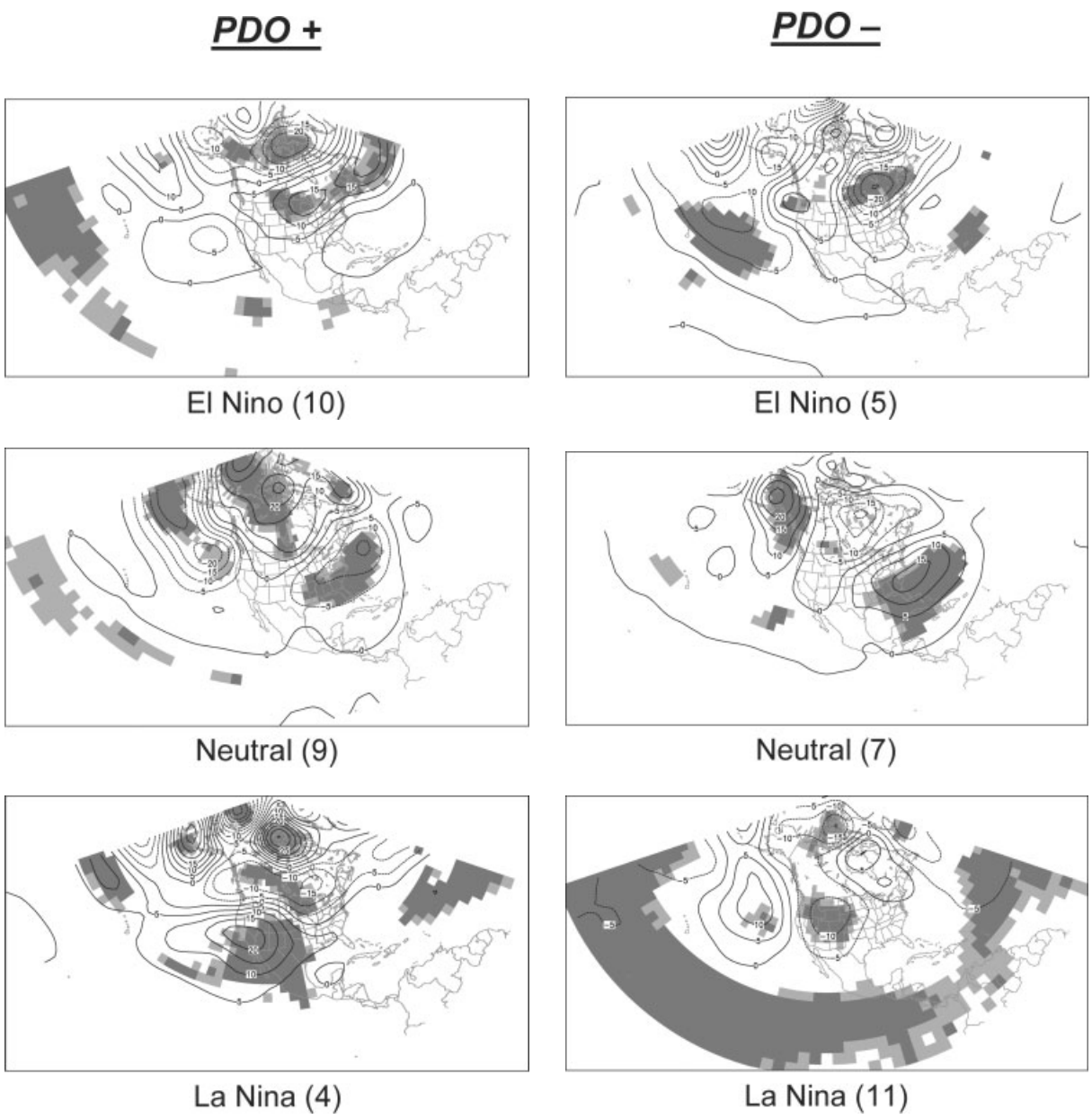

Figure 6. May 700 mb geopotential height anomaly composites by PDO and ENSO phase subgroups (solid lines, positive anomaly; dashed lines, negative anomalies; contour interval, 5 m). Dark shading indicates significance at 0.05 level and light shading indicates significance at 0.10 level. Numbers in parentheses represent number of years used in each composite group.

The El Niño-PDO− composite was similar to the El Niño-PDO+ composite with subtle shifts in the highest and lowest geopotential height anomalies. The negative geopotential height anomaly off of the California coast was significant, but shifted further west towards Hawaii. Positive geopotential height anomalies shifted towards the northwest United States and negative geopotential height anomalies dominated the area south of Hudson Bay in east-central Canada.

The anomaly patterns associated with each PDO phase are made up of different numbers and types of ENSO events. El Niño conditions were present for 10 of the 23 years in the PDO+ composite, whereas 11 of the 23 years in the PDO− composite were La Niña conditions. This is especially evident with the PDO− composite (Figure 5). The positive–negative geopotential height anomaly pattern in the La Niña-PDO− composite is very similar to the overall PDO− composite, but it is stronger and produces significant anomalies. This tendency towards more La Niña events during the negative PDO phase and El Niño events during the positive phase helps explain the overall shift to more May exceedance days during PDO− and less during PDO+.

3.4. Teleconnection patterns

It is unclear what the exact mechanisms are that either limit or promote the development of the negative geopotential height anomaly pattern characterized by the daily exceedance composite in Figure 2 during the transition

season month of May. The neutral and El Niño sub-composites of PDO+ have negative geopotential height anomalies of the California coast, which may be remnants of the Aleutian Low, a semi-permanent and key winter circulation feature in the North Pacific. A strong Aleutian Low is associated with the positive phase of the PDO and typically shifts east during El Niño events (Gershunov and Barnett, 1998; Niebauer 1998; Overland *et al*., 1999). Composite analysis of several El Niño events performed by Overland *et al*. (2001) showed that the strong, wintertime Aleutian Low ended quickly in April, but negative geopotential height anomalies persisted into June over the North Pacific south of the original low centre. These anomalies may be due to the changes in SST patterns over the North Pacific induced by the Aleutian Low that persists into the spring. The negative anomalies do not appear to be strong enough to represent persistent, blocking features, but may be a weak forcing mechanism for positive geopotential height anomalies downstream over the western United States counter to the critical fire weather pattern in Figure 2.

The positive geopotential height anomalies over the southwest United States during La Niña-PDO+ do appear to represent a blocking pattern that would weaken the geopotential height gradient associated with extreme fire weather days as identified in Crimmins (2006). A pattern of positive geopotential height anomalies in May would tend to push the springtime baroclinic zone across the western United States further north away from Arizona and New Mexico. La Niña events were relatively rare during the positive PDO phase of the study period with only 4 years in the La Niña-PDO+ group. There appears to be relatively strong agreement in the geopotential height anomaly patterns between the 4 years, but they account for only 9% of the total years during the study period.

The La Niña-PDO− and neutral-PDO− represent 78% of the total years comprising PDO−. Both of these sub-composites have positive geopotential height anomalies over the eastern Pacific region and negative anomalies over the western United States consistent with the exceedance day composite in Figure 2. Burnett (1994) found that upstream positive geopotential height anomalies over the eastern Pacific were a consistent feature associated with the development of negative height anomalies over the southwest United States. Weak, wintertime Aleutian Lows are associated with the negative phase of the PDO. The weaker than normal Aleutian Low may condition North Pacific SSTs that directly or indirectly promote positive geopotential height anomalies that persist into the spring.

The constructive phasing suggested by Gershunov and Barnett (1998) with negative PDO-La Niña and positive PDO-El Niño events having the most stable teleconnection patterns appears to only be valid for the La Niña-PDO− group in this study. This group has the most exceedance days of any group and also has a significant positive–negative geopotential height anomaly pattern similar to the exceedance day composite pattern. The El Niño-PDO+ does not have a strong anomaly pattern that would help explain its fewer than expected exceedance days. The destructive pairing of La Niña and PDO+ actually has the strongest anomaly pattern and the pattern explains the fewer than expected observations in this group, but has a very small sample size and should be interpreted with caution.

3.5. Connections to southwestern wildfire variability

Much research has documented the relationship between ENSO variability and changes in southwestern United States precipitation regimes during the winter months (Redmond and Koch, 1991; Gershunov, 1998; Cayan *et al*., 1999). El Niño (La Niña) events tend to bring above (below) normal precipitation to the Southwest during the winter months of December-January-February-March (DJFM). Recent research has also shown that the stability of this teleconnection is dependent on the phase of the PDO (Gershunov and Barnett, 1998; Gutzler *et al*., 2002; Brown and Comrie, 2004). The negative (positive) phase of the PDO tends to bring more La Niña (El Niño) events and an extended number of years with below (above) normal winter precipitation (Gray *et al*., 2003).

Regional-scale wildfire variability across the Southwest has been linked to the low-frequency climate variability inherent in the ENSO teleconnection patterns discussed earlier. Swetnam and Betancourt (1998) used ENSO to help explain periodic wildfire events in xeric forests across Arizona and New Mexico following sequences of El Niño and La Niña events. They hypothesized that wet winters associated with El Niño events were promoting the growth of fine fuels and suppressing fires while subsequent dry, La Niña winters helped to condition fuels. The sequence of climatic conditions that promote fuel growth and fuel drying would culminate in fire seasons with high total area burned.

The results of this study indicate that the low-frequency wet-dry cycles associated with ENSO may not be the only climatic components modulating fire season activity across the southwest United States. Changes in the frequency of regional-scale extreme fire weather events appear to change with the same low-frequency components related to ENSO and PDO. La Niña events that typically bring dry winters to the Southwest also are related to a higher frequency of extreme fire weather events in May when the PDO is in the negative phase. Changes in the frequency of extreme fire weather conditions appear to be more dependent on the longer term shifts related to the PDO. The last several decades were characterized by the positive phase of the PDO, several of the strongest El Niño events on record, and exceptionally wet winters across the Southwest. This period has brought unprecedented surges in biomass across the United States, exacerbating already high fuel loadings (Swetnam and Betancourt, 1998). A return to the negative PDO phase would mean not only an extended period of drier conditions but also a higher frequency of extreme

fire weather conditions during the fire season. This combination could lead to catastrophic wildfire seasons with a shift to a more consistent negative PDO phase.

4. Conclusions

Low-frequency changes in North Pacific SSTs related to the PDO appear to modulate the frequency of May regional-scale extreme fire weather events across the southwest United States. Extreme event frequencies were significantly different from expected for both positive PDO and negative PDO years. More May events (69) occurred during negative PDO conditions than during positive PDO conditions (32).

Subgroups of PDO phases (positive and negative) based on ENSO state provide further insight into the connection between Pacific Ocean SST anomalies and southwestern United States critical fire weather patterns. La Niña events during the negative phase of the PDO had the highest total number of exceedance days of any subgroup. About 700 mb geopotential height anomaly composites identified a significant positive–negative height anomaly pattern over the eastern Pacific-western United States that is favourable for the development of extreme fire weather conditions over the Southwest.

In general, La Niña and neutral ENSO conditions during PDO− had positive geopotential height anomalies over the eastern Pacific that may either not block the development of negative geopotential height anomalies over the western United States or actually enhance them. This pattern appears to be favourable for developing the steep geopotential height gradients across the Southwest necessary for extreme fire weather conditions (Crimmins, 2006). El Niño events during both phases of PDO had weak negative geopotential height anomalies over the eastern Pacific and were associated with fewer than expected exceedance days. La Niña events during the positive PDO phase produced a significant positive geopotential height anomaly across Arizona and New Mexico weakening the geopotential height gradient associated with extreme fire weather days across the region. This subgroup was associated with only two exceedance days when 8.8 were expected.

The higher than expected frequencies associated with La Niña-PDO− events and the negative PDO phase in general have important ramifications for the southwest United States. The exceptionally wet period from 1977 to 1998 associated with extreme El Niño events and a generally positive PDO phase may switch soon to a more consistent negative PDO phase. This shift may not only bring drier winter conditions as expected but also increasing the extreme fire weather activity during the spring. The combination of long-term fuel accumulation spurred on by the wet period of 1976–2001, below normal precipitation and consequent drying of fine fuels in upcoming winters and more frequent hot, dry and windy spring days could mean a substantial increase in extreme wildfire activity across the southwest United States in the coming decade.

Acknowledgements

This research was funded in part by a NASA Space Grant Graduate Fellowship. The author wishes to thank Beth Hall and Hauss Reinbold for the great amount of assistance they provided in obtaining the RAWS data critical for this study. Many thanks also to Theresa Crimmins, Andrew Comrie, Katie Hirschboeck, Thomas Swetnam, Tim Brown, Gregg Garfin and two anonymous reviewers who all provided constructive feedback that improved the final article.

References

Brotak EA, Reifsnyder WE. 1977. An investigation of the synoptic situations associated with major wildland fires. *Journal of Applied Meteorology* **16**: 867–870.

Brown DP, Comrie AC. 2004. A winter precipitation 'dipole' in the western United States associated with multi-decadal ENSO variability. *Geophysical Research Letters* **31**: L09203.1–L09203.4.

Burnett AW. 1994. Regional-scale troughing over the southwestern United States: temporal climatology, teleconnections, and climatic impact. *Physical Geography* **15**: 80–98.

Cayan DR, Redmond KT, Riddle JG. 1999. ENSO and hydrologic extremes in the western United States. *Journal of Climate* **12**: 2881–2893.

Climate Prediction Center. 2010. ENSO Impacts: Oceanic Niño Index. Climate Prediction Center. http://www.cpc.noaa.gov/products/analysis_monitoring/ensostuff/ensoyears.shtml (access year 2010).

Crimmins M, Comrie A. 2004. Wildfire-climate interactions across southeast Arizona. *International Journal of Wildland Fire* **13**: 455–466.

Crimmins MA. 2006. Synoptic climatological analysis of extreme fire weather conditions across the southwest United States. *International Journal of Climatology* **26**: 1001–1016.

Efron B, Tibshirani R. 1993. *An Introduction to the Bootstrap*. Chapman & Hall: New York.

Flannigan MD, Stocks BJ, Weber WG. 2003. Fire regimes and climatic change in Canadian forests. In *Fire and Climatic Change in Temperate Ecosystems of the Western Americas*. Veblen TT, Baker WL, Montenegro G, Swetnam TW (eds). Springer-Verlag: New York.

Fosberg MA. 1978. Weather in wildland fire management: the fire weather index. *Conference on Sierra Nevada Meteorology*. American Meteorological Society: Lake Tahoe, CA.

Fosberg MA, Mearns L, Price C. 1993. Climate change – fire interactions at the global scale: predictions and limitations of methods. In *Fire in the Environment: The Ecological, Atmospheric, and Climatic Importance of Vegetation Fires*. Crutzen PJ, Goldammer JG (eds). John Wiley & Sons: Chichester.

Gershunov A. 1998. ENSO influence on intraseasonal extreme rainfall and temperature frequencies in the contiguous United States: implications for long-range predictability. *Journal of Climate* **11**: 3192–3203.

Gershunov A, Barnett TP. 1998. Interdecadal modulation of ENSO teleconnections. *Bulletin of the American Meteorological Society* **79**: 2715–2725.

Goodrick SL. 2002. Modification of the Fosberg fire weather index to include drought. *International Journal of Wildland Fire* **11**: 205–211.

Gray ST, Betancourt JL, Fastie CL, Jackson ST. 2003. Patterns and sources of multidecadal oscillations in drought-sensitive tree-ring records from the central and southern Rocky Mountains. *Geophysical Research Letters* **30**: 49.1–49.4.

Gutzler DS, Kann DM, Thornbrugh C. 2002. Modulation of ENSO-based long-lead outlooks of southwestern U.S. winter precipitation by the Pacific Decadal Oscillation. *Weather and Forecasting* **17**: 1163–1172.

Haines DA, Main WA, Frost JS, Simard AJ. 1983. Fire-danger rating and wildfire occurrence in the northeastern United States. *Forest Science* **29**: 679–696.

Hidalgo HG, Dracup JA. 2003. ENSO and PDO effects on hydroclimatic variations of the upper Colorado River basin. *Journal of Hydrometeorology* **4**: 5–23.

Johnson EA, Wowchuk DR. 1993. Wildfires in the southern Canadian Rocky Mountains and their relationship to mid-tropospheric anomalies. *Canadian Journal of Forest Research* **23**: 1213–1222.

Kalnay E, Kanamitsu M, Kistler R, Collins W, Deaven D, Gandin L, Iredell M, Saha S, White G, Wallen J, Zhu Y, Leetmaa A, Reynolds B, Chelliah M, Ebisuzaki W, Higgins W, Janowiak J, Mo KC, Ropelewski C, Wang J, Jenne R, Joseph D. 1996. The NCEPNCAR 40-Year Reanalysis project. *Bulletin of the American Meteorological Society* **77**(77): 437–471.

Littell JS, McKenzie D, Peterson DL, Westerling AL. 2009. Climate and wildfire area burned in western U.S. ecoprovinces, 1916–2003. *Ecological Applications* **19**: 1003–1021.

Mantua N, Hare S, Zhang Y, Wallace J, Francis R. 1997. A Pacific interdecadal climate oscillation with impacts on salmon production. *Bulletin of the American Meteorological Society* **78**: 1069–1079.

McCabe GJ, Dettinger MD. 1999. Decadal variations in the strength of ENSO teleconnections with precipitation in the western United States. *International Journal of Climatology* **19**: 1399–1410.

Nash CH, Johnson EA. 1996. Synoptic climatology of lightning-caused forest fires in subalpine and boreal forests. *Canadian Journal of Forest Research* **26**: 1859–1874.

Niebauer HJ. 1998. Variability in Bering Sea ice cover as affected by a regime shift in the North Pacific in the period 1947–1996. *Journal of Geophysical Research* **102**: 27,717–27,737.

Overland JE, Adams JM, Bond NA. 1999. Decadal variability of the Aleutian Low and its relation to high-latitude circulation. *Journal of Climate* **12**: 1542–1548.

Overland JE, Bond NA, Adams JM. 2001. North Pacific atmospheric and SST anomalies in 1997: links to ENSO? *Fisheries Oceanography* **10**: 69–80.

Redmond KT, Koch RW. 1991. Surface climate and streamflow variability in the western United States and their relationship to large-scale circulation indices. *Water Resources Research* **77**: 2391–2399.

Schlobohm PM, Brain J. 2002. *Gaining an Understanding of the National Fire Danger Rating System*. National Wildfire Coordinating Group: Boise, ID.

Schroeder MJ. 1969. *Critical Fire Weather Patterns in the Conterminous United States*. Environmental Science Services Administration: Silver Spring, MD.

Sheppard PR, Comrie AC, Packin GD, Angersbach K, Hughes MK. 2002. The climate of the U.S. Southwest. *Climate Research* **21**: 219–238.

Simard AJ, Haines DA, Main WA. 1985. Relations between El Niño/Southern Oscillation anomalies and wildland fire activity in the United States. *Agricultural and Forest Meteorology* **36**: 93–104.

Swetnam TW, Betancourt JL. 1990. Fire-Southern Oscillation relations in the southwestern United States. *Science* **249**: 1017–1020.

Swetnam TW, Betancourt JL. 1998. Mesoscale disturbance and ecological response to decadal climatic variability in the American Southwest. *Journal of Climate* **11**: 3128–3147.

Swets JA. 1988. Measuring the accuracy of diagnostic systems. *Science* **240**: 1285–1293.

Takle ES, Bramer DJ, Heilman WE, Thompson MR. 1994. A synoptic climatology for forest fires in the NE US and future implications from GCM simulations. *International Journal of Wildland Fire* **4**: 217–224.

Trenberth KE. 1997. The definition of El Niño. *Bulletin of the American Meteorological Society* **78**: 2771–2777.

Westerling AL, Cayan DR, Brown TJ, Hall BL, Riddle JG. 2004. Climate, Santa Ana Winds and Autumn Wildfires in Southern California. *EOS* **85**: 289–296.

Westerling AL, Swetnam TW. 2003. Interannual to decadal drought and wildfire in the western United States. *EOS* **84**: 4.

